ORIGINAL RESEARCH

Synthesized zinc peroxide nanoparticles (ZnO$_2$-NPs): a novel antimicrobial, anti-elastase, anti-keratinase, and anti-inflammatory approach toward polymicrobial burn wounds

Sameh Samir Ali[1,2,*]
Reda Morsy[3,4,*]
Nessma Ahmed El-Zawawy[2]
Mervat F Fareed[5,6]
Mohamed Yaser Bedaiwy[2]

[1]Biofuels Institute, School of the Environment and Safety Engineering, Jiangsu University, Zhenjiang, China; [2]Botany Department, Faculty of Science, Tanta University, Tanta, Egypt; [3]Physics Department, Faculty of Science, Tanta University, Tanta, Egypt; [4]Physics Department, Faculty of Dentistry, Al Baha University, Al Baha, Saudi Arabia; [5]Department of Home Economic, Faculty of Specific Education, Tanta University, Tanta, Egypt; [6]Department of Biology, Faculty of Science, Taif University, Taif, Saudi Arabia

*These authors contributed equally to this work

Abstract: Increasing of multidrug resistance (MDR) remains an intractable challenge for burn patients. Innovative nanomaterials are also in high demand for the development of new antimicrobial biomaterials that inevitably have opened new therapeutic horizons in medical approaches and lead to many efforts for synthesizing new metal oxide nanoparticles (NPs) for better control of the MDR associated with the polymicrobial burn wounds. Recently, it seems that metal oxides can truly be considered as highly efficient inorganic agents with antimicrobial properties. In this study, zinc peroxide NPs (ZnO$_2$-NPs) were synthesized using the co-precipitation method. Synthesized ZnO$_2$-NPs were characterized by X-ray diffraction, Fourier transformed infrared, transmission electron microscopy, thermogravimetric analysis, differential scanning calorimetry, and ultraviolet-visible spectroscopy. The characterization techniques revealed synthesis of the pure phase of non-agglomerated ZnO$_2$-NPs having sizes in the range of 15–25 nm with a transition temperature of 211°C. Antimicrobial activity of ZnO$_2$-NPs was determined against MDR *Pseudomonas aeruginosa* (PA) and *Aspergillus niger* (AN) strains isolated from burn wound infections. Both strains, PA6 and AN4, were found to be more susceptible strains to ZnO$_2$-NPs. In addition, a significant decrease in elastase and keratinase activities was recorded with increased concentrations of ZnO$_2$-NPs until 200 μg/mL. ZnO$_2$-NPs revealed a significant anti-inflammatory activity against PA6 and AN4 strains as demonstrated by membrane stabilization, albumin denaturation, and proteinase inhibition. Moreover, the results of in vivo histopathology assessment confirmed the potential role of ZnO$_2$-NPs in the improvement of skin wound healing in the experimental animal models. Clearly, the synthesized ZnO$_2$-NPs have demonstrated a competitive capability as antimicrobial, anti-elastase, anti-keratinase, and anti-inflammatory candidates, suggesting that the ZnO$_2$-NPs are promising metal oxides that are potentially valued for biomedical applications.

Keywords: co-precipitation method, burn wound infections, metal oxides nanoparticles, multidrug resistance, antimicrobial, anti-inflammatory

Introduction

Increasing multidrug resistance (MDR) has generated scientific interest to synthesize novel antimicrobial agents with broad spectrum activities to complement and/or replace conventional antibiotics.[1] There are two main categories of antimicrobial agents, organic and inorganic. Over the past decade, inorganic materials, such as metal and metal oxides, have attracted more attention as they have been found to be safe for human beings and animals and also had the efficiency to withstand harsh conditions.[2]

Correspondence: Sameh Samir Ali
Biofuels Institute, School of the Environment and Safety Engineering, Jiangsu University, Zhenjiang 212013, Jiangsu, China
Tel +86 150 6149 1030
Email samh_samir@science.tanta.edu.eg

To date, several types of synthetic metal oxide nanoparticles (NPs), such as titanium, silver, zinc, ferric, silicon, copper, and magnesium oxide have profound antimicrobial activities. The inorganic zinc oxide nanoparticles (ZnO-NPs) are of particular interest because of their unique properties, such as antibacterial, antifungal, wound healing, good chemical stability, biocompatibility, and low toxicity.[3–6] ZnO-NPs may be considered as bi-functional materials because of their ability to work as safe antimicrobial agents for dermatological and orthopedic applications in addition to the role of zinc as a vital trace element for building, stabilizing, and functioning of proteins and enzymes.[7,8] Moreover, most of the elements constituting the metal oxides are considered as trace elements that are vital to the human body.[9] Therefore, there is a great interest in incorporating antimicrobial metal oxide NPs within orthopedic, dental, and skin biomaterials.[10,11] Synthesis of metal oxide NPs using wet chemical methods is an interesting nanotechnology field because wet chemical methods are economic and simple.[12] The antimicrobial activity of metal oxides has been strongly associated with their morphology, particle size, and surface area.[13] For example, metal oxide particles of smaller size, no greater than 100 nm, and larger surface area have exhibited stronger antimicrobial activity due to their capability to interact and damage the microbial membranes.[14,15]

Burn wounds are considered a huge public health issue all over the world, especially in the developing countries. Microbial infections in burn wound patients are common and are difficult to control. In Egypt, nosocomial infection requires more attention than it currently receives. It constitutes a major problem due to morbidity and mortality among hospitalized patients. In addition to the lack of universal approach, unavailability of records, statistics as well as information, makes the problem difficult to control.[16] Approximately, 50%–75% of morbidity in hospitalized burn patients is due to microbial infections.[17] Microbial infection is one of the most serious complications that happen in the acute period following burn.[18] Polymicrobial communities (biofilms) are consortia of bacteria and fungi that colonize the damaged tissues and secrete polysaccharides that provide an optimal environment for polymicrobial survival. Polysaccharide biofilm is an important barrier to microbial consortia, enabling their escape from host immunity and confers increased tolerance to antimicrobials when compared with monomicrobial infections.[19,20] Moreover, the increase in MDR is due to the strong antibiotic selective pressure from the clinical and environmental origin. The most common etiological bacteria attributed to chronic burn wound infections are *Pseudomonas*

aeruginosa, Staphylococcus aureus, Streptococcus spp., *Klebsiella* spp., *Enterococcus* spp., and *Escherichia coli*. The most prevalent fungi are *Aspergillus niger, Candida* spp. in addition to the genera of *Aureobasidium, Malassezia, Curvularia, Ulocladium*, and *Trichophyton*.[21,22] Limited reports have documented the bacterial and fungal co-interactions, which are often found together in different environments.[23] The contribution of fungal pathogens to polymicrobial biofilms is more than 50% in the majority of the burn wound infections.[24] Recently, the bacterial-fungal co-infection caused by *S. aureus* and *Candida albicans* revealed a unique architecture when *S. aureus* was associated with fungal hyphae. Interestingly, a number of virulence factors in *S. aureus* were enhanced by *C. albicans*.[25] Burns caused by both *P. aeruginosa* and *S. aureus* have resulted in a chronic non-healing wound in which such co-infection have shown that the *P. aeruginosa* limits *S. aureus* growth.[26] The majority of previous studies on polymicrobial burn infections have documented the pathogen-infection interaction, but often ignored the host microbiota. Grice et al[27] reported that the presence of host microbiota-associated pathogens in burns could lower the efficiency of burn healing.

The microbial enzyme is a virulence weapon, acts as a part of pathogen lifestyle in the infection establishment. Elastases and keratinases secreted by bacteria and fungi were investigated to help in skin invasion during burns.[28] Elastase (small serine protease) is a protein-degrading enzyme, including elastin substrate. It is an endopeptidase, which catalyzes the hydrolysis of internal peptide bonds within the protein. Elastin is an insoluble and highly cross-linked protein of connective tissues.[29] Elastase as one member of the chymotrypsin family of proteases has a tissue-damaging activity, which is primarily responsible for the breakdown of elastin and capable of degrading various plasma proteins during infections as in *P. aeruginosa*.[26,30] Furthermore, keratinases are an arsenal of proteases secreted by some bacterial and fungal pathogens,[31,32] that disseminate through the stratum corneum and subsequently digest the keratin network into absorbable amino acids. Dermatophytosis is a dermatophyte superficial infection in keratinized skin, caused by secretion of multiple serine-subtilisins and fungalysins (keratinases). The role of these enzymes is to reduce disulfide bonds in keratins of skin, which facilitate the penetration into host cellular system.[33] Indeed, keratinases are the major causal agents of tinea diseases. Our literature survey indicates that no available reports documented the activity of microbial elastases and/or keratinases in burn-causing infections, or reducing their activities by using metal oxide NPs. Therefore,

this is the first study to evaluate the efficiency of synthesized ZnO$_2$-NPs as anti-elastase and anti-keratinase.
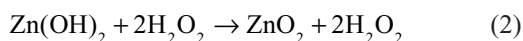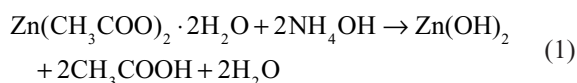
Inflammation reaction is the response of living tissues to injury. During this process, lysosomal enzymes produce a variety of disorders, by which macromolecules damaging and membrane lipid peroxidation are assumed to be responsible for certain pathological conditions.[34] Therefore, stabilization of lysosomal membrane is important in limitation of the inflammatory response. The mechanism of anti-inflammation depends on inhibiting the release of lysosomal constituents of activated neutrophil such as proteases, bactericidal, and fungicidal enzymes, which cause further damage and tissue inflammation upon lysosomal membrane stabilization or by extracellular releasing.[34] Anti-inflammatory activity of ZnO-NPs has been previously reported.[35] However, to the best of the authors' knowledge, to date, there have been no reports to discuss the anti-inflammatory activity of zinc peroxide nanoparticles (ZnO$_2$-NPs) for further in vivo application as a novel ointment in the treatment of burn wounds.

Difficulties in the management of burn infection beside much attention toward other safe biologically active compounds have become an interesting research field and integral part of modern medical applications, and also encourage researchers to develop inorganic antimicrobial agents based on metal oxide NPs.[36,37] Therefore, the aim of the present study is to design and characterize ZnO$_2$-NPs as a novel antimicrobial, anti-elastase, anti-keratinase, and anti-inflammatory approach combating polymicrobial MDR pathogens of burn wound infections.

Material and methods
Synthesis of ZnO$_2$-NPs
ZnO$_2$-NPs were essentially synthesized using the following analytical grade chemicals without further purification: zinc acetate dihydrate (Zn[CH$_3$COO]$_2$·2H$_2$O), ammonium hydroxide (NH$_4$OH), hydrogen peroxide (H$_2$O$_2$; sol 40%), glycerol, ethanol, and acetone (Adwic, El-nasr Chemical Co., Cairo, Egypt). An aqueous suspension of ZnO$_2$-NPs was synthesized in a typical procedure by using the following co-precipitation route,

$$Zn(CH_3COO)_2 \cdot 2H_2O + 2NH_4OH \rightarrow Zn(OH)_2 \\ + 2CH_3COOH + 2H_2O \quad (1)$$

$$Zn(OH)_2 + 2H_2O_2 \rightarrow ZnO_2 + 2H_2O_2 \quad (2)$$

In a typical procedure, NH$_4$OH (10 mL) was mixed with 20 mL of 0.1 mol of Zn(CH$_3$COO)$_2$·2H$_2$O under magnetic stirring. Immediately, 70 mL of acetone and 3 g glycerol were rapidly added to the suspension. Then 40 mL of H$_2$O$_2$ was added to the suspension with stirring at room temperature for 30 min. The suspended precipitate was centrifuged and washed 3 times with distilled water.[38–40]

Characterization of ZnO$_2$-NPs
ZnO$_2$-NPs were characterized by various conventional methods. The crystalline structure ZnO$_2$-NPs were characterized by X-ray diffraction (XRD) using a Philips PW 1840 diffractometer (Mahwah, NJ, USA). CuKα radiation of 1.5406Å wavelength at 40 kV and 30 mA was used to expose the samples through a Ni filter. The 2θ values were set in the range of 10°–65°. Peaks on the X-ray patterns recorded for the sample were compared with standard XRD pattern of ZnO$_2$ (Joint Committee on Powder Diffraction Standards [JCPDS] card No 13-0311). The mean crystallite size was calculated using the Scherer equation. Fourier transformed infrared (FT-IR) spectrum was obtained with Perkin-Elmer-1430 (Perkin Elmer, Waltham, MA, USA) using KBr pellet technique for the range 4.000 and 400 cm^{-1}. The nanostructures and size distribution of the synthetic particles were examined by transmission electron microscopy (TEM) using a JEM 100SX (JEOL, Co., Akishima, Japan) operating at an acceleration voltage of 80 kV. The specimens for TEM investigations were prepared by placing a drop of ZnO$_2$ suspension on a carbon-coated copper grid (400 mesh; Electron Microscopy Sciences, Hatfield, PA, USA) and allowing this to dry in air under ambient conditions. Thermal behavior of synthetic ZnO$_2$ was analyzed using differential scanning calorimetry (DSC, Shimadzu DSC-60A) and thermo-gravimetric analyzer (TGA, a Shimadzu TGA-50) at a heating rate of 10°C/min under a nitrogen atmosphere. The ultraviolet-visible (UV-vis) spectrum of the ZnO$_2$ suspension was measured by using UV-vis recording spectrophotometer (Unico-2800s).[41]

Isolation, identification, and selection of dominant polymicrobial pathogens
A total of 47 swabs of burn wounds were kindly provided by the Clinical Laboratories of Burn Units at Tanta University Hospitals and El-Menshawy Hospitals. All burn wound patients provided written informed consent, and the study protocol was approved by the review board of Tanta University Hospitals and El-Menshawy Hospitals for the collection of swabs from the Laboratories of Burn Units. The clinicians followed the guidelines and the standard protocols that are compatible with the requirements of the Declaration of Helsinki. The swabs were transferred to the Lab of Microbiology

at Faculty of Science, Tanta University, Egypt, and immediately inoculated on selective and non-selective culture media. The identified isolates were sent to the hospital labs for diagnosis. For isolation of bacteria, the swabs were cultured on blood agar, cetrimide agar, chocolate agar, MacConkey agar, and nutrient agar (Sigma, St Louis, MO, USA). The swabs were inoculated on various mycological media (Sabouraud's dextrose agar "Pharmacopoeia, New York, USA" with and without gentamicin and chloramphenicol and also on blood agar) for isolation of fungi. All plates were incubated under aerobic conditions for up to 72 h. Monomicrobial and polymicrobial cultures were recorded. Moderate or heavy growth was regarded as a positive culture, whereas sparse growth was neglected. Phenotypic identification and conventional biochemical tests for bacteria and fungi were performed.[42–44] Moreover, isolated yeasts were identified according to the protocols.[45,46] In order to confirm the phenotypic observation of *P. aeruginosa* and *A. niger* from polymicrobial cultures, *P. aeruginosa* were re-inoculated on cetrimide agar supplemented with 15 µg/mL nalidixic acid and checked by using VITEK® 2 automated systems (BioMérieux, Marcy-L'E'toile, France). The strains of *A. niger* were grown on potato dextrose agar medium at 30°C for 7 days. The color and mycelial growth were observed daily. In addition, the spores-producing *A. niger* was identified up to the genus and species level based on macroscopic and microscopic criteria[44] as shown in supplementary additional files (Figure S1).

Antimicrobial susceptibility test for selecting MDR strains

Antibiotic susceptibility test was performed by disc diffusion method.[47] Agar plates of Muller-Hinton (Sigma) and Sabouraud's dextrose were prepared for bacteria and fungi, respectively. For inoculum preparation, *P. aeruginosa* was cultured on nutrient agar and incubated for overnight. Then, it was suspended in sterile normal saline solution. The bacterial concentration was adjusted to 1×10^7 colony-forming units (CFUs)/mL. *A. niger* was incubated for 7 days at 30°C on Sabouraud's dextrose agar. The conidial suspensions were prepared according to the basic fungicidal activity test EN 1275.[48] The density of conidia in the spore suspension was optically adjusted to a concentration of (1×10^7 CFU/mL). The prepared bacterial and fungal inocula were swabbed on the top surface of Muller-Hinton agar and Sabouraud's dextrose agar media, respectively, and then allowed to dry for 10 min. The antibacterial and antifungal discs (Table 1) were placed aseptically on the surface of the inoculated agar plates and left for 15 min at room temperature for diffusion. All plates were then incubated for 18 h at 37°C for bacteria and 30°C for fungi for up to 3 days. The sensitivity was determined by measuring the zone of growth inhibition (mm) around the discs. The results were interpreted according to the Clinical and Laboratory Standards Institute standards.[49] MDR was defined as resistance to at least 3 or more antimicrobial categories.

Antimicrobial activity of ZnO₂-NPs

In vitro antimicrobial activity of synthesized ZnO_2-NPs was carried out by disc diffusion method as mentioned above. Different concentrations (200, 100, and 50 µg/mL) of ZnO_2-NPs-impregnated filter paper discs (6 mm) were tested against MDR *P. aeruginosa* and *A. niger* strains. Minimum inhibitory concentration (MIC) was performed by a serial dilution technique[50] using 96-well microtiter plates. Various concentrations (200, 100, 50, 25, 12.5, 6.25, and 3.12 µg/mL) of ZnO_2-NPs were prepared, and 2 µL of the prepared inoculum solution was added to every well. The plates were incubated at the optimal conditions for bacteria and fungi. MIC was the lowest concentration of ZnO_2-NPs at which no visible growth was observed. For determining minimum bactericidal concentration (MBC) and minimum fungicidal concentration (MFC), a volume of the aliquots (10 µL) from the tubes, which was used in MIC assays and showed no turbidity, was sub-cultured on the surface of the nutrient agar and Sabouraud's dextrose agar for bacteria and fungi, respectively. MBC was defined as the lowest concentration of the ZnO_2-NPs at which there was no colony formation of *P. aeruginosa* after 18 h incubation period, while MFC was regarded as the lowest concentration of ZnO_2-NPs that did not yield *A. niger* growth after days of the incubation period.

Elastase activity

The selected bacterial and fungal strains were cultured in Luria-Bertani agar and Sabouraud's dextrose agar plates, respectively. The freshly prepared cultures were then inoculated onto agar plates containing 0.15% elastin (Sigma). The plates were incubated at 37°C for 24 h for bacteria and at 30°C for 72 h for fungi. The formation of proteolytic halo clear zone around colony is a positive result of elastase production.[51] Elastase-producing strains were selected for quantitative assay as determined by diazocoupling method,[52] using succinyl-L-alanyl-L-alanyl-L-alanyl-p-nitroanilide (STANA) (Sigma) as a substrate and measuring p-nitroanilide (p-NA) released from STANA. One unit of elastase is defined as the amount of p-NA released from STANA at 1 min.

Elastase inhibition by ZnO_2-NPs was determined spectrophotometrically using STANA as the substrate by monitoring

Table 1 Antimicrobial activity of ZnO₂-NPs against MDR *Pseudomonas aeruginosa* and *Aspergillus niger* strains

Strain number	Diameter of inhibition zone (mm) Concentrations of ZnO₂-NPs (µg/mL)			MIC	MBC	MFC	AMP
	50	100	200				
PA1	7.0±0.0[a]	7.0±0.0[a]	8.0±0.0[a]	50	100	ND	AX, CTX, CAZ, CRO, ATM, SXT, TE, C, K, CT
PA2	0.0±0.0[b]	0.0±0.0[b]	0.0±0.0[b]	ND	ND	ND	AX, CTX, CAZ, FEP, CRO, ATM, CIP, SXT, TE, C, TOB, K
PA3	9.0±1.0[c]	10.0±1.0[c]	11.0±1.0[c]	50	100	ND	AX, CTX, CAZ, ATM, CIP, SXT, TE, C, K, CT
PA4	7.0±1.0[a]	12.0±0.0[d]	15.0±2.0[d]	25	50	ND	AX, CAZ, FEP, CRO, CIP, SXT, CN, TOB, K, CT
PA5	0.0±0.0[b]	0.0±0.0[b]	0.0±0.0[b]	ND	ND	ND	AX, CTX, CAZ, FEP, CRO, CIP, SXT, TE, K
PA6	12.0±2.0[d]	17.0±2.0[e]	21.0±1.0[e]	6.25	12.5	ND	AX, CTX, CAZ, CRO, ATM, CIP, SXT, TE, CN, TOB, K, CT
PA7	9.0±0.0[c]	13.0±0.0[d]	18.0±0.0[f]	6.25	12.5	ND	AX, CTX, CAZ, CRO, ATM, IPM, SXT, TE, C, TOB, CT
PA8	10.0±1.0[e]	11.0±1.0[d]	15.0±1.0[d]	25	50	ND	AX, CTX, CAZ, FEP, CRO, ATM, CIP, SXT, C, K, CT
PA9	7.0±0.0[a]	9.0±0.0[f]	12.0±0.0[c]	50	100	ND	AX, CAZ, FEP, ATM, CRO, IPM, CIP, SXT, C, CN, TOB, K, CT
PA10	0.0±0.0[b]	0.0±0.0[b]	0.0±0.0[b]	ND	ND	ND	AX, CTX, CAZ, FEP, ATM, CIP, SXT, TE, C, CN, TOB, K, CT
PA11	0.0±0.0[b]	7.0±0.0[a]	10.0±1.0[c]	50	100	ND	AX, CTX, CAZ, FEP, CRO, ATM, CIP, SXT, TE, TOB, K, CT
AN1	20.0±2.0[f]	25.0±1.0[g]	35.0±3.0[g]	6.25	ND	12.5	ITC, MIZ, FLC, NYT, TRB
AN2	10.0±0.0[e]	16.0±1.0[e]	22.0±2.0[e]	12.5	ND	25	ITC, CLT, FLC, MCFG, TRB
AN3	0.0±0.0[b]	0.0±0.0[b]	0.0±0.0[b]	0.0	ND	ND	AMB, ITC, MIZ, FLC, MCFG, TRB
AN4	30.0±3.0[g]	30.0±3.0[h]	40.0±1.0[h]	6.25	ND	12.5	ITC, CLT, FLC, MCFG, NYT, TRB
AN5	20.0±2.0[f]	25.0±2.0[g]	30.0±2.0[i]	6.25	ND	12.5	AMB, ITC, CLT, MIZ, FLC, TRB
AN6	11.0±0.0[h]	11.0±0.0[d]	18.0±0.0[f]	25	ND	50	ITC, CLT, MIZ, FLC, NYT, TRB
AN7	14.0±2.0[i]	20.0±1.0[i]	25.0±1.0[j]	6.25	ND	12.5	AMB, ITC, CLT, FLC, MCFG, NYT, TRB
AN8	9.0±0.0[c]	16.0±1.0[e]	20.0±0.0[e]	25	ND	50	AMB, ITC, MIZ, FLC, TRB
AN9	18.0±2.0[j]	22.0±2.0[i]	32.0±2.0[g,i]	6.25	ND	12.5	ITC, CLT, MIZ, FLC, MCFG, TRB
AN10	14.0±1.0[i]	20.0±1.0[i]	28.0±1.0[j]	25	ND	50	AMB, ITC, CLT, MIZ, FLC, NYT, TRB
AN11	0.0±0.0[b]	0.0±0.0[b]	0.0±0.0[b]	0.0	ND	ND	ITC, CLT, FLC, MCFG, NYT, TRB
ANOVA							
F	0.133	0.0349	0.001				
P-value	0.875	0.965	0.998				

Notes: Values are the mean of three replicates ± SD. Means with the same letters in the same column show the insignificant difference ($P \leq 0.05$).
Abbreviations: AMB, amphotericin; AMP, antimicrobial profile; AN, *Aspergillus niger*; ANOVA, analysis of variance; ATM, aztreonam; AX, amoxicillin; C, chloramphenicol; CAZ, ceftazidime; CIP, ciprofloxacin; CLT, clotrimazole; CN, gentamicin; CRO, ceftriaxone; CT, colistin sulfate; CTX, cefotaxime; FEP, cefepime; FLC, fluconazole; IPM, imipenem; ITC, itraconazole; K, kanamycin; MBC, minimum bactericidal concentration; MCFG, micfungin; MDR, multidrug resistance; MFC, minimum fungicidal concentration; MIC, minimum inhibitory concentration; MIZ, miconazole; NPs, nanoparticles; ND, not detected; NYT, nystatin; PA, *Pseudomonas aeruginosa*; SXT, cotrimoxazole; TE, tetracycline; TOB, tobramycin; TRB, terbinafine.

the release of p-NA at 550 nm. Briefly, elastase crude enzyme was incubated together with different concentrations of ZnO₂-NPs. After 15 min of pre-incubation at 37°C, 20 µL of 50 mM substrate STANA was added to 0.9 mL of 50 mM Tris/HCl buffer, pH 7.5. Absorbance was measured for 60 min after addition of STANA. The inhibition activity was calculated after stopping the reaction using 1 mL of 10% trichloroacetic acid (TCA). To the reaction mixture, 0.2 mL of 0.1% sodium nitrate, 0.5% ammonium sulfamate, and 0.1% N-(1-naphthyl) ethylenediamine dihydrochloride were added and the color developed was determined spectrophotometrically at 550 nm.

Keratinase activity

The keratin-degrading capability was investigated as described by Wawrzkiewicz et al[53] with some modifications using keratin powder (Sigma) instead of chicken feathers,

which was considered as a keratin source. The agar plates of feather meal medium (0.01% Mg₂SO₄, 0.14% K₂HPO₄, 0.07% KH₂PO₄, 0.05% NaCl, 1.0% ground keratin, 1.5% Bacto agar) were inoculated with freshly prepared inocula of tested bacterial and fungal strains. The keratolytic activity of the strains was observed as a halo clear zone surrounding the colony. Keratinase activity of keratinase-producing strains was quantitated spectrophotometrically according to the method of Joshi et al[54] with some modifications, using azokeratin as the substrate. Briefly, an aliquot (800 µL) of the substrate azokeratin (5 mg dissolved in 50 mM phosphate buffer pH 7.5) was added to a 1.5 mL centrifuge tube. To this reaction mixture, 200 µL of the appropriately diluted crude supernatant enzyme was mixed. After 60 min of incubation at 50°C in water bath shaker, the reaction was stopped by adding 200 µL of 15% (w/v) TCA. The reaction mixture was centrifuged at 10,000 *g* for 15 min. The optical absorption of

the supernatant was measured at 450 nm against the blank (without TCA). The increase in absorbance (A450) by 0.01 was considered as one unit (1 U) of keratinase activity when compared with the control. This formula (total activity [U/mL] = Δ OD/0.01) was used for calculation of keratinase activity. Keratinase inhibition was determined spectrophotometrically using the substrate azokeratin after incubation of the keratinase crude enzyme together with different concentrations of ZnO_2-NPs as described.[54]

Anti-inflammatory activity
Membrane stabilization
The anti-inflammatory activity of ZnO_2-NPs was determined by human red blood cells membrane stabilization (HRBCsMS) method with some modifications.[55,56] Briefly, blood samples were collected from healthy volunteers who provided written informed consent, and the collection of blood samples from the healthy volunteers was approved by the review board of Tanta University Hospitals and El-Menshawy Hospitals. The blood was centrifuged at 3,000 rpm and packed cells were washed twice with normal saline solution (0.85%, pH 7.0) and 10% v/v suspension was prepared with normal saline. The assay reaction mixture contained 1 mL of ZnO_2-NPs at different concentrations and 1 mL of freshly prepared 10% human red blood cells (HRBCs) suspension. Normal saline solution (2 mL) was used as a control. Aspirin (Bayer, Leverkusen, Germany) was used as the reference drug. The assay mixture was incubated at 56°C for 30 min and centrifuged at 2,500 rpm for 5 min. The supernatant solution, which contained hemoglobin, was estimated spectrophotometrically at 560 nm. The percentage of hemolysis was calculated by assuming that 100% hemolysis resulted in the presence of normal saline solution. The percentage of HRBCsMS was calculated according to the following formula:

$$\% \text{ HRBCsMS} = 100 - \left(\frac{\text{OD of sample tested}}{\text{OD of control}} \right) \times 100$$

Albumin denaturation
To assay albumin denaturation, different concentrations of ZnO_2-NPs were mixed with 1% aqueous solution of bovine albumin (Merck, Darmstadt, Germany) fraction. The mixtures were incubated at 37°C for 20 min, then heated at 51°C for 20 min. The turbidity was measured spectrophotometrically at 660 nm. Aspirin was used as the reference drug.[57,58] The protection of protein denaturation (%) was calculated according to the following formula.[59,60] One hundred percent is the denaturation that resulted in the presence of distilled water.

$$\% \text{ Protection} = 100 - \left(\frac{\text{OD of sample tested}}{\text{OD of control}} \right) \times 100$$

Proteinase inhibitor activity
To assay trypsin inhibition, 0.06 mg trypsin (dissolved in 1 mL of 20 mM Tris-HCl buffer, pH 7.4) was mixed together with varying concentrations of ZnO_2-NPs to a final volume of 2 mL. After incubation for 5 min at 37°C, 1 mL of 0.8% azocasein (Sigma) in 20 mM $NaHCO_3$, pH 8.1 was added to the reaction mixture at 37°C for 20 min. The reaction was stopped by adding 2 mL of 10% (w/v) TCA solution. The assay mixture was centrifuged at 12,000 g for 10 min, then 2 mL of 1.0 M NaOH was mixed to the supernatant and absorbance was measured at 440 nm against the buffer as a blank.[61] The percentage of proteinase inhibitory activity was calculated as mentioned above.

Skin burn wounds
New Zealand white rabbits were investigated to evaluate ZnO_2-NPs in the healing of their dermal burn wounds in this study. The animal experiment protocol was reviewed and approved by the Institutional Animal Ethics Committee (IAEC), Faculty of Science, Tanta University, Egypt (code; Rec-Sci-Tu-020) and the procedures in the present study were performed in accordance with the IAEC guidelines. The experimental design, ointment formulation, and the protocol of anesthesia and sacrifice were explained in detail in our previous paper.[62] The back of rabbits was shaved, injected intramuscularly with ketamine (Vetoquinol, Lavaletrie, Canada) (15 mg/kg) and xylazine (1.1 mg/kg) to induce sedation before burning. The burn was produced by applying a hot square spatula of 1 cm^2 surface area, which had been heated on the flame, to the shaved backs of the rabbits for 30 s. The selected strains *P. aeruginosa* (PA6) and *A. niger* (AN4), which isolated from the patients of infected burn wounds, were used to induce infection in the burned areas of the experimental animal models. The freshly prepared cultures were used to prepare the inoculum in normal saline solution, and the microbial concentration was adjusted spectrophotometrically. The same volume of a bacterial and fungal suspension of 1×10^7 CFU/mL was applied to the inflamed areas. The rabbits were randomly divided into 4 groups (n=6). Group 1 (negative control) in which rabbits were burnt, did not get infected or receive any treatment. Group 2 (positive control) in which rabbits were burnt, infected, but did not receive any treatment. Group 3 (ZnO_2-NPs-receiving group) in which rabbits were burnt, microbial suspensions were applied, and the rabbits received treatment with ZnO_2-NPs ointment. Group 4 (silver sulfadiazine-receiving group) in

which rabbits were burnt, microbial suspensions were applied, and received treatment with silver sulfadiazine ointment (Dermazin; Sandoz, Princeton, NJ, USA). The formulation of ZnO$_2$-NPs ointment was prepared as described.[63] Skin biopsies were taken on seventh, fourteenth, and twenty-first days and clinical evaluation, including the degree of healing and wound area size, was performed macroscopically and histopathologically. The biopsy samples (0.5×1.5 cm^2) were fixed in a buffered formaldehyde solution (10%). The paraffin block sections were prepared and stained with hematoxylin for histopathological examinations.

Statistical analysis

Results are presented as the mean ± standard deviation of 3 replicates. The statistical analyses were carried out using SPSS-20. The obtained data were analyzed statistically to determine the degree of significance using one-way analysis of variance and Student's t-test at a probability level $P\leq0.05$.

Results and discussion
Characterization of ZnO$_2$-NPs

XRD pattern has been used to confirm that synthetic ZnO$_2$-NPs have the same crystal structure of standard ZnO$_2$ particles. Figure 1 shows XRD pattern of the synthetic ZnO$_2$-NPs produced by co-precipitation method. XRD pattern of ZnO$_2$-NPs did not detect any impurity peaks and revealed a pure single phase structure that coincided with that of standard cubic ZnO$_2$ crystal structure (JCPDS card No 13-0311). XRD pattern reveals strong XRD reflections at $2\theta=37.2°$ and $62.2°$ for plans (200), and (311), respectively suggesting the formation of ZnO$_2$-NPs with good crystal quality. The broadening of the XRD reflections indicated that the synthesized ZnO$_2$ particles are in the nanometer range where the average crystallite size of synthetic ZnO$_2$-NPs was about 13 nm as calculated by the Scherer's equation: $D = k.\lambda/$

($\beta.\cos\theta$), where $k=0.9$; λ is the wavelength of monochromatic X-ray radiation ($\lambda=1.5406$ Å), θ is the Bragg, angle and β is the full width of X-ray pattern line at half peak.

The FT-IR spectrum of synthetic ZnO$_2$-NPs is shown in Figure 2. The spectrum reveals characteristic infrared absorption bands at 3,450, 2,370, 1,645, 1,390, and 1,050 cm^{-1} that attributed to the vibrations of Zn-O. The absorbed H$_2$O on the surface of ZnO$_2$-NPs revealed the presence of two infrared (IR) bands: one at 3,450 cm^{-1}, belonging the stretching vibration of the O-H bond, and the another at 1,645 cm^{-1} belonging the bending vibration of H-O-H.[38] FT-IR spectrum does not show any of absorption bands of -COO or -CH$_3$ groups of zinc acetate, suggesting the purity of synthetic ZnO$_2$-NPs.[41] Figure 3 shows TEM images of synthetic ZnO$_2$-NPs. It demonstrates the possibility of precise determination of spherical ZnO$_2$-NPs; the particles are well-defined and well dispersed non-agglomerated NPs having spherical structures with average particle sizes in the range of 15–25 nm. The results indicate that synthetic ZnO$_2$-NPs have well-dispersed ZnO$_2$-NPs. The average particle sizes determined by TEM images were very close to the crystallite size calculated from XRD results.

The TGA and DSC curves, Figure 4, showed the thermal behavior of synthetic ZnO$_2$-NPs from room temperature, 25°C up to 500°C. The TGA curve shows weight losses in temperatures ranging from 25°C to 500°C; a weight loss of about 4.2% below 100°C, solid arrows in Figure 4, owing to adsorbed water on the surface of ZnO$_2$ particles, a weight loss of about 8.7% up to 16°C owing to removal of adsorbed and chemisorbed water, and an abrupt weight loss of about 14.9%, from 92.3% to 77.4%, in the temperature range from 165°C to 245°C and then remains almost constant up to 500°C. This drop confirms the transformation of ZnO$_2$ to ZnO.

The DSC curve revealed an exothermic peak at 211°C that is in agreement with abrupt weight loss in TGA curve,
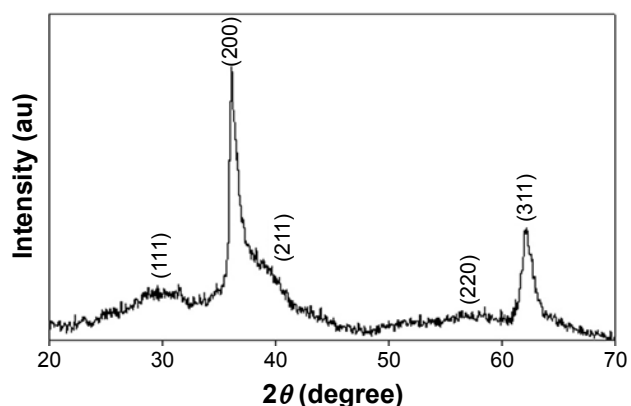

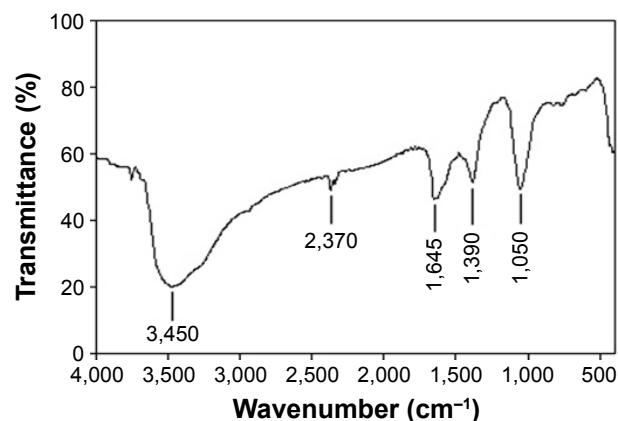**Figure 1** X-ray diffraction pattern of the synthetic ZnO$_2$-NPs.

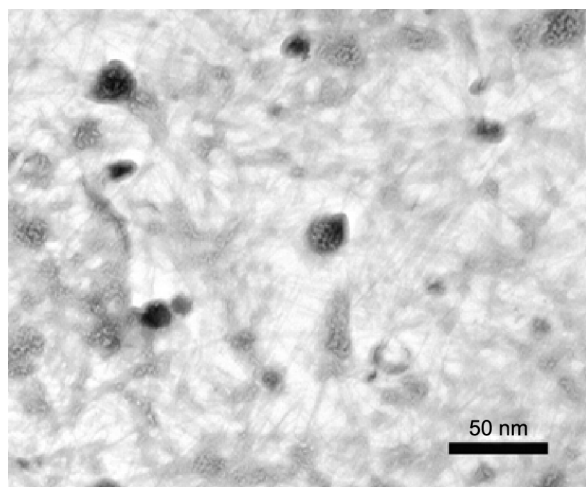**Figure 2** Fourier transformed infrared spectrum of the synthetic ZnO$_2$-NPs.

Figure 3 Transmission electron microscopy image of the synthetic ZnO$_2$-NPs.

Figure 5 Ultraviolet spectra of the synthetic ZnO$_2$-NPs.

which is attributed to oxygen release due to decomposition of ZnO$_2$ molecules to ZnO and oxygen, according to the following chemical reaction equation,

$$2\,ZnO_2 = 2\,ZnO + O_2 \qquad (3)$$
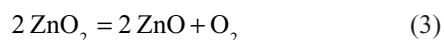
After decomposition temperature, 211°C, up to 500°C, the formed ZnO has a stable hexagonal phase.[41] Figure 5 demonstrates the UV-vis spectrum of synthetic ZnO$_2$-NPs suspension. The synthetic ZnO$_2$-NPs have an optical UV absorption in the region (200–300 nm), with maximum absorption occurring at 239 nm.

Incidence of monomicrobial and polymicrobial infections

Out of 47 clinical swabs recovered from skin burn wounds, polymicrobial infections were recorded in 28 patients (59.6%), while the remaining cases yielded monomicrobial
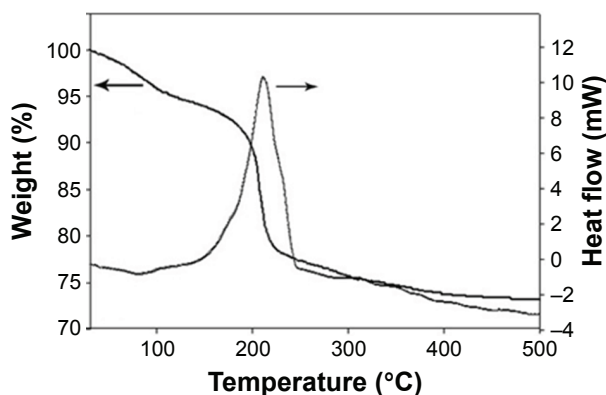
infection. Out of 28 patients who had polymicrobial cultures, mixed bacteria alone were recorded in 5 (17.8%) patients, mixed fungi alone were isolated from 6 patients (21.4%), and mixed bacteria and fungi were recorded in 17 patients (60.7%). The predominant bacteria and fungi were *P. aeruginosa* and *A. niger*, respectively, and observed in 11 (64.7%) patients, while other mixed bacteria and fungi were recorded in the remaining 6 patients (33.3%). Mousa[64] reported that polymicrobial bacterial and fungal burn wound infections were observed in 57.5%. *P. aeruginosa* was the most common isolate (19.1%) and the predominant fungi were *Aspergillus* sp. Our results are in coincidence with results from previous studies.[65–69] Martin et al[20] found that the presence of one microorganism generates an appropriate environment for other pathogenic microorganisms, which are able to colonize the respective niche, so 2 or more pathogenic microorganisms could synergically interact to cause disease.

Figure 4 Thermogravimetric analysis and differential scanning calorimetric curves of the synthetic ZnO$_2$-NPs.

Multidrug resistance and antimicrobial profile (AMP)

All strains of *P. aeruginosa* and *A. niger* were tested against 15 antibacterial agents and 8 antifungals. The AMP of each strain tested is presented in Table 1. From these results, we concluded that all strains were MDR. Among the β-lactams used against *P. aeruginosa*, all strains were found to be resistant to amoxicillin and ceftazidime. Moreover, the incidence of resistance against cefotaxime, ceftriaxone, and aztreonam were 81.8%, while 63.6% of these bacterial strains exhibited resistance to cefepime. In addition to β-lactam antibiotics, the *P. aeruginosa* strains also exhibited a higher incidence of resistance to non-β-lactams. Maximum resistance was

recorded to co-trimoxazole (100%), followed by kanamycin (90.9%), colistin sulphate (81.8%), tetracycline (72.7%), ciprofloxacin (72.7%), tobramycin (63.6%), gentamicin (36.4%), and imipenem (18.2%). Indeed, all *A. niger* strains were resistant to itraconazole, fluconazole, and terbinafine. Maximum resistance was found to clotrimazole (72.7%), miconazole (54.5%), micafungin (54.5%), nystatin (54.5%), and amphotericin (45.4%). Data of AMP revealed that all of the tested *P. aeruginosa* and *A. niger* strains demonstrated phenotypic resistance to at least 3 different classes of antibacterial and antifungal agents, and were classified as MDR *P. aeruginosa* and *A. niger*. Recently, the accumulated misuse and overuse of anti-infectious drugs have led to the development of MDR-resistant strains. Pathogens developed, by the acquisition of resistance genes or genetic mutations, defense mechanisms that made them difficult to treat, resulting in prolonged illness with a greater risk of death. At the moment, nanotechnology-based drug delivery systems emerged as a promising approach to circumvent the limitations of conventional drugs to assess the safety, quality, and efficacy.[70] Therefore, in the near future, nanotechnology could play a key role against MDR clinical pathogens.

Antimicrobial activity of ZnO$_2$-NPs against MDR strains

There are several reports, which have investigated ZnO-NPs due to their unique properties, such as antibacterial, antifungal, and wound healing.[71] The present study is might be the first to investigate ZnO$_2$-NPs against polymicrobial MDR pathogens isolated from burn wound infections. Antimicrobial activities of synthesized ZnO$_2$-NPs were tested against MDR *P. aeruginosa* and *A. niger* (Table 1). The ZnO$_2$-NPs show significant inhibitory activity against strains tested with distinct differences in the susceptibility to ZnO$_2$-NPs in a dose-dependent manner. The mean zones of inhibition ranged from 7.0±0.0 to 40.0±1.0 mm. *P. aeruginosa* (PA6) and *A. niger* (AN4) strains were found to be more susceptible strains to ZnO$_2$-NPs. The highest mean zones of inhibition ranged from 12.0±2.0 to 21±1.0 mm and from 30.0±3.0 to 40±1.0 mm against PA6 and AN4, respectively. Five strains (PA2, PA5, PA10, AN3, and AN11) showed no sensitivity against ZnO$_2$-NPs even at its high concentration (200 µg/mL). MIC, MBC, and MFC are shown in Table 1. The values of MIC ranged between 6.25 and 50 µg/mL. MBC values ranged between 12.5 and 100 µg/mL, while MFC from 12.5 to 50 µg/mL. The antimicrobial activities of ZnO$_2$-NPs against MDR bacterial and fungal clinical pathogens depend on particle size, the concentration of the

powder, morphology, and specific surface area. The increase in ZnO$_2$-NPs concentration (50, 100, and 200 µg/mL) correlated with increasing antimicrobial activities. This may be due to the increased H$_2$O$_2$ concentration from the surface of ZnO$_2$. By this way, the generated H$_2$O$_2$ can penetrate the cell membranes of *P. aeruginosa* and *A. niger*, and kill them. Sangeetha and Kumaraguru[72] explained the mechanism of antimicrobial activities of metal oxide NPs. The small particle size of metal oxide NPs is associated with a larger band gap; consequently, these unfavorable conditions can prevent the recombination of excitons. Therefore, more available excitons will result in the formation of a higher concentration of reactive oxygen species, and consequently enhance the antimicrobial activities of metal oxide NPs.[72]

ZnO$_2$-NPs as anti- elastase and anti-keratinase

A number of virulence factors are secreted by *P. aeruginosa* and can contribute to its pathogenicity. Current antifungal therapy has been threatened by the development of MDR strains, in addition to host toxicity of available polyenes as well as the fungistatic mode of azoles action.[73] Targeting pathogenicity and virulence are now considered valuable approaches against clinical pathogens.[74] Therefore, discovering novel drugs with enhanced efficacy, safety, and/or alternative mode of combating infections is needed. Establishment of microbial pathogenesis depends on the host-cell interaction with virulence factors secretion, mainly proteinases, including elastase (LasB protease), keratinases, lipases, gelatinases, and phospholipases. These proteinases virulence factors are extracellular enzymes, probably essential for establishing bacterial and fungal infections to degrade structural barrier, in addition to obtaining nutrients.[75] PA6 and AN4 strains were examined for qualitative production of elastase and keratinase on agar plates, and they were able to produce extracellular elastase and keratinase enzymes. The enzyme activity was assessed based on the observation of a clear zone.

Recent trends in the screening of alternative antimicrobial agents against MDR pathogens prompted us to evaluate the efficacy of ZnO$_2$-NPs as an anti-virulent active agent against MDR *P. aeruginosa* and *A. niger*. Elastases and keratinases production is reported to aid in the pathogenesis of *P. aeruginosa* and *Aspergillus* sp. [75,76] and, therefore, proteinase inhibitors are being explored as potential antibacterial and antifungal agents. PA6 and AN4 strains were assessed quantitatively for the production of elastase and keratinase enzymes (Figure 6). PA6 showed relatively higher production
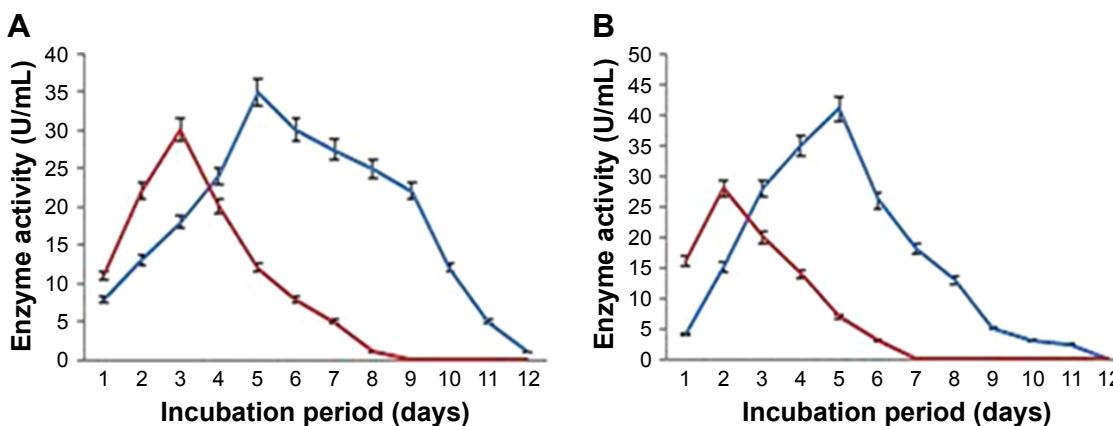
Figure 6 Time course of elastase (**A**) and keratinase (**B**) production by PA6 strain (blue line) and AN4 strain (red line).
Abbreviations: AN, *Aspergillus niger*; PA, *Pseudomonas aeruginosa*.

of elastase (30 U/mL) and keratinase (28 U/mL) on the third day and second day of growth, respectively. In addition, the highest production of elastase and keratinase was observed on the fifth day of growth, and recorded at 35 and 41 U/mL, respectively, for the AN4 strain. From these results, ZnO_2-NPs were tested for their anti-elastase and anti-keratinase activity against both PA6 and AN4 strains (Table 2). A significant decrease in elastase and keratinase activities was recorded with increased concentrations of ZnO_2-NPs until 200 µg/mL, at which enzyme activities completely stopped. Proteinases are believed to contribute to microbial virulence by digesting immunologically important proteins and destroying host tissues.[77] As well, the inhibition of these enzyme activities may reduce the microbial pathogenesis. Therefore, the broad spectrum anti-proteinase activities of ZnO_2-NPs in addition to growth inhibition of PA6 and AN4 are indicative of the efficacy of ZnO_2-NPs as potential antibacterial and antifungal drugs. To the best of the authors' knowledge, to date, there

have been no reports to evaluate the efficacy of ZnO_2-NPs as anti-elastase and anti-keratinase activity against mixed bacterial and fungal pathogens isolated from burn wound infections.

In vitro anti-inflammatory activity of ZnO_2-NPs

Anti-inflammatory activity of ZnO_2-NPs was performed to explore its efficiency. The inhibitory activity of ZnO_2-NPs (100–2,000 µg/mL) was evaluated through membrane stabilization, albumin denaturation, and proteinase inhibitory activity compared with commercially available aspirin (Table 3). Also, ZnO_2-NPs showed significant stabilization toward human red blood cells membrane (HRBCsM). Moreover, the percentage protection of ZnO_2-NPs at concentration 2,000 µg/mL was highly similar to that of a standard anti-inflammatory drug (aspirin) at the same concentration with maximum inhibition 81% and 82.1% caused by ZnO_2-NPs and aspirin, respectively (Table 3). Other studies reported the membrane stabilization method for studying in vitro anti-inflammatory activity due to the similarity between erythrocyte membrane and lysosomal membrane.[78,79] The stabilization implies that the ZnO_2-NPs may well stabilize lysosomal membranes.

Albumin denaturation is another mechanism to explore the efficiency of ZnO_2-NPs as an anti-inflammatory active agent. Protein denaturation is a process through which proteins lose their secondary and tertiary structure as well as their biological function by application of external stress. In addition, protein denaturation is a well-documented cause of inflammation. A significant increase in inhibiting albumin denaturation was observed by increasing the concentrations of ZnO_2-NPs and aspirin until 2,000 µg/mL. However, ZnO_2-NPs were effective in inhibiting albumin denaturation with

Table 2 Anti-elastase and anti-keratinase activities of ZnO_2-NPs

Concentration of ZnO_2-NPs (µg/mL)	Enzyme activity (U/mL)			
	Elastase		Keratinase	
	PA6	AN4	PA6	AN4
6.25	28.0±1.0[a]	31.0±1.0[a]	25.0±1.0[a]	37.0±2.0[a]
12.5	23.0±2.0[b]	21.0±1.0[b]	13.0±1.0[b]	35.0±1.0[b]
25	18.0±1.0[c]	14.0±0.0[c]	9.0±0.0[c]	26.0±0.0[c]
50	6.0±0.0[d]	8.0±0.0[d]	5.0±0.0[d]	20.0±1.0[d]
100	1.0±0.0[e]	2.0±0.0[e]	0.0±0.0[e]	12.0±0.0[e]
200	0.0±0.0[f]	0.0±0.0[f]	0.0±0.0[e]	0.0±0.0[e]
ANOVA				
F	0.002	0.001	0.002	0.007
P-value	0.997	0.998	0.997	0.992

Notes: Values are the mean of three replicates ± SD. Means with the same letters in the same column showed the insignificant difference ($P \leq 0.05$).
Abbreviations: AN, *Aspergillus niger*; ANOVA, analysis of variance; NPs, nanoparticles; PA, *Pseudomonas aeruginosa*.

Table 3 Anti-inflammatory effect of ZnO$_2$-NPs compared to aspirin

Concentration (µg/mL)	Inhibitory percentage of albumin denaturation		Percentage of membrane stabilization activity		Inhibitory percentage of proteinase activity	
	ZnO$_2$-NPs	Aspirin	ZnO$_2$-NPs	Aspirin	ZnO$_2$-NPs	Aspirin
100	25.0±0.0[a]	40.1±0.7[a]	28.0±1.0[a]	42.3±1.1[a]	30.0±0[a]	58.0±1.0[a]
250	40.0±2.0[b]	41.7±1.1[a,b]	45.0±1.0[b]	68.6±1.5[b]	47.0±2[b]	68.7±2.2[b]
500	57.0±3.0[c]	45.7±2.5[b]	62.0±2.0[c]	71.3±2.0[b]	58.0±2[c]	81.5±0.5[c]
1,000	82.0±1.0[d]	71.1±1.0[c]	73.0±1.0[d]	74.9±0.5[b,c]	80.0±1[d]	83.7±0.4[c]
2,000	90.0±3.0[d]	85.3±2.1[d]	81.0±3.0[e]	82.1±2.2[c]	89.0±2[e]	89.2±1.9[c]
ANOVA						
F	0.0008	0.0004	0.0156	0.045	0.0003	0.0193
P-value	0.9991	0.9995	0.9845	0.9561	0.9996	0.9808

Notes: Values are the mean of three replicates ± SD. Means with the same letters in the same column showed the insignificant difference ($P \leq 0.05$).
Abbreviations: ANOVA, analysis of variance; NPs, nanoparticles.

maximum inhibition of 90% when compared with aspirin, which showed 85.3% maximum inhibition (Table 3).

Anti-inflammatory activity of ZnO$_2$-NPs was also conducted by proteinase inhibitory mechanism. Lysosomic neutrophils are a rich source of serine proteinase. Das and Chatterjee[80] reported that leukocytes proteinase plays a key role in the development of tissue damage during inflammation as well as a significant role of protection provided by proteinase inhibitors. In the present study, ZnO$_2$-NPs exhibited a significant anti-proteinase activity. Also, ZnO$_2$-NPs were similar to aspirin in the inhibition of proteinase. The maximum inhibition for both was reached 89% at 2,000 µg/mL (Table 3). It might be the first study to discuss the in vitro anti-inflammatory activity of ZnO$_2$-NPs. Therefore, we suggest it as a lead compound for designing an alternative drug with a potent anti-inflammatory activity in the treatment of skin burn wounds. Hence, new in vivo treatment was conducted in order to evaluate the feasibility of ZnO$_2$-NPs in curing the skin wound infections, which can avoid the problem of increasing MDR bacterial and fungal pathogens if treated by conventional antibiotics.

In vivo histopathological evaluation of ZnO$_2$-NPs

At the beginning (first day) of the in vivo evaluation, the average diameter of the rabbit's skin burns was 1.5±0.3 cm. All model groups were controlled during the 3 weeks of the experiment, and the rate of wound healing was measured. Topical application of ZnO$_2$-NPs in the group of rabbits receiving ZnO$_2$-NPs enhanced the rate of wound healing significantly (0.3±0.1 cm), compared with the other groups. It was observed that the rabbits in this group had no ulcers compared with positive control and sulfadiazine-receiving. Both groups 2 and 4 showed large open burn wounds with

no significant increase in wound diameter of 1.1±0.2 cm and 1.3±0.1 cm, respectively. In the healing process, the damaged, burned tissues were restored to their normal status through several clinical mechanisms, including the contraction of wound that helped shrinkage of the damaged wound area. In addition, the rate of healing depended on the ability of the damaged tissues to repair themselves. The commercial synthetic ointment (silver sulfadiazine) in the case of burn treatment proved to be an effective antibacterial and antifungal agent; however, its drawback is that it delays the healing process by inhibiting the proliferation of the fibroblast and keratinocytes; this also leads to impairment of the healing process.[81,82] According to the antibiogram patterns of the isolated polymicrobial strains of *P. aeruginosa* and *A. niger* from patients of the infected burn wounds, all the bacterial and fungal strains were MDR, and according to the results of ZnO$_2$-NPs activities, PA6 and AN4 strains were selected as a mixed inoculum for induction of infection during in vivo evaluation of ZnO$_2$-NPs as promising antimicrobial agents against MDR pathogens in infected burn wounds. According to our results, the silver sulfadiazine ointment-receiving group showed no improvement in the treatment of infected burn, and this may be due to no eradications of PA6 and AN4 from the burn wounds that were more serious than rabbits of group 2 (positive control), which were infected by PA6 and AN4 strains without burn treatment. On the other hand, ZnO$_2$-NPs-receiving group exhibited a significant reduction in the burn surface area as well as skin contraction, which was almost complete. Furthermore, the rabbits of group 1 (negative control, burnt and without induction or treatment) were better than those of positive control group.

Histopathological microscopic examinations of all rabbit groups are shown in Figure 7 and in Supplementary materials (Table S1). Histopathological examination of wound healing
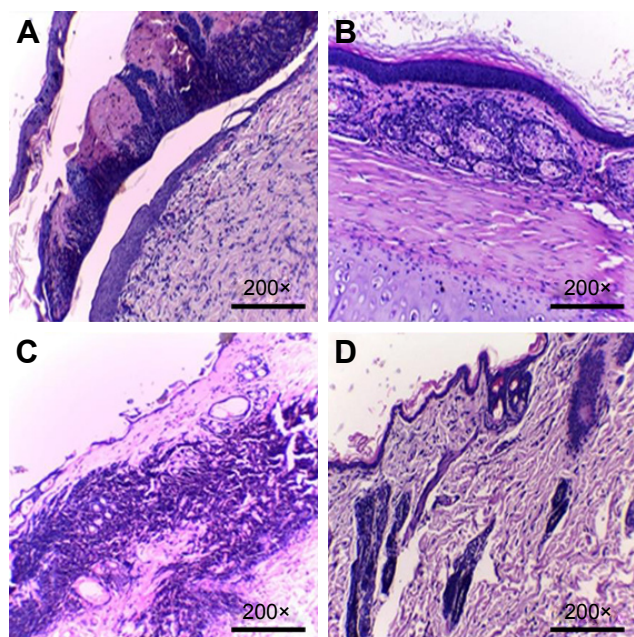
Figure 7 Histopathological examination of burn wounds after 7 days (**A**, **C**) and 21 days (**B**, **D**) after treatment protocols with ZnO$_2$-NPs (**A**, **B**) compared to silver sulfadiazine (**C**, **D**).
Note: Magnification power (200×).
Abbreviation: NPs, nanoparticles.

in the ZnO$_2$-NPs-receiving group compared with silver sulfadiazine-receiving group revealed that the surface ulceration significantly decreased in the rabbit group receiving ZnO$_2$-NPs, whereas the seventh day of treatment showed ulcer healing with creeping of epithelium tissue by new healthy tissue to cover the ulcerated area. In addition, after 21 days of treatment, the ZnO$_2$-NPs-receiving group showed complete healing with a complete surface re-epithelialization, and no evidence of surface ulceration was observed (Figure 7A and B). On the other hand, after 21 days of treatment of burned skin in the silver sulfadiazine-receiving group, microscopic examination revealed delayed re-epithelialization, surface ulceration, inflammatory infiltrate, and congested vessels (Figure 7C and D). According to these results, ZnO$_2$-NPs have been proven to have a great potential toward MDR microorganisms-infecting burns. Therefore, we suggest the use of ZnO$_2$-NPs as an alternative or additional method of treatment of burn wounds infected with polymicrobial pathogens, such as *P. aeruginosa* and *A. niger*. Indeed, further studies should be conducted to well establish the efficiency of ZnO$_2$-NPs in clinical practices.

Conclusion

The synthesis of a nanotechnology-based antimicrobial system is an expanding research area, which can contribute to the development of novel technologies, especially

against MDR pathogens. ZnO$_2$-NPs were synthesized via co-precipitation method by oxidation of precipitated ZnO particles in the presence of H$_2$O$_2$ as oxidizing agent, and glycerol as a surface modifier to prevent agglomeration of NPs. Also, XDR pattern of ZnO$_2$-NPs confirmed a pure single phase with cubic ZnO$_2$ crystal, which compared with JCPDS card No 13-0311. FT-IR spectrum does not show any of absorption bands of −COO or −CH$_3$ groups of zinc acetate, suggesting the purity of synthetic ZnO$_2$-NPs. The characterization techniques using TEM revealed synthesis of the pure phase of non-agglomerated ZnO$_2$-NPs having spherical shape with sizes in the range of 15–25 nm. In addition, ZnO$_2$-NPs have a transition temperature of 211°C. Antimicrobial activities of ZnO$_2$-NPs increased with the increase of concentrations. Moreover, our results reported the reduced virulence and pathogenicity of both MDR strains, PA6 and AN4, by showing a reduction in their elastase and keratinase activities. Furthermore, the anti-inflammatory activity of ZnO$_2$-NPs was comparable with standard aspirin. Our findings provide scientific evidence to support clinical uses of ZnO$_2$-NPs, which have a great promising potential for the development of an anti-inflammatory agent. Indeed, in vivo histopathological results exhibited that ZnO$_2$-NPs may be effective as promising antimicrobial agents against MDR *P. aeruginosa* and *A. niger* inhabiting burn wounds. More investigations are needed on human volunteers with skin burns to confirm the efficacy of ZnO$_2$-NPs as a novel antimicrobial drug in wound healing, especially after the success of ZnO$_2$-NPs in the treatment of burn wounds of the experimental animal models compared with silver sulfadiazine ointment.

Author contributions

Conceived and designed the experiments: SSA, RM, NAZ, and MFF. Performed the experiments: SSA, RM, and NAZ. Analyzed the data: SSA, RM, NAZ, MFF, and MB. Contributed reagents/materials/analysis tools: SSA, RM, NAZ, and MB. Contributed to the writing of the manuscript: SSA, RM, NAZ, MFF, and MB.

Disclosure

The authors report no conflicts of interest in this work.

References

1. Wang L, Hu C, Shao L. The antimicrobial activity of nanoparticles: present situation and prospects for the future. *Int J Nanomedicine*. 2017; 12:1227–1249.
2. Jacob SP, Bharathkumar R, Ashwathram G. *Aspergillus niger* mediated synthesis of ZnO nanoparticles and their antimicrobial and in vitro anticancerous activity. *World J Pharm Res*. 2014;3(2):3044–3054.
3. Zhao J, Fan B, Wu Z, et al. Serum zinc is associated with plasma leptin and Cu–Zn SOD in elite male basketball athletes. *J Trace Elem Med Bio*. 2015;30:49–53.
4. Cui H, Wu X, Chen Y, et al. Influence of copper doping on chlorine adsorption and antibacterial behavior of MgO prepared by co-precipitation method. *Mate Res Bull*. 2015;61:511–518.
5. Samanta PK. Review on wet chemical growth and anti-bacterial activity of zinc oxide nanostructures. *J Tissue Sci Eng*. 2017;8:1.
6. Padmavathy N, Vijayaraghavan R. Enhanced bioactivity of ZnO nanoparticles – an antimicrobial study. *Sci Technol Adv Mater*. 2008; 9:035004.
7. Şeker S, Elçin AE, Yumak T, et al. In vitro cytotoxicity of hydrothermally synthesized ZnO nanoparticles on human periodontal ligament fibroblast and mouse dermal fibroblast cells. *Toxicol In Vitro*. 2014; 28(8):1349–1358.
8. Fielding G, Bose S. SiO₂ and ZnO dopants in three-dimensionally printed tricalcium phosphate bone tissue engineering scaffolds enhance osteogenesis and angiogenesis in vivo. *Acta Biomaterialia*. 2013; 9(11):9137–9148.
9. Kabata-Pendias A, Mukherjee AB. *Trace Elements from Soil to Human*. Berlin, Heidelberg: Springer; 2007.
10. Vargas-Reus MA, Memarzadeh K, Huang J, et al. Antimicrobial activity of nanoparticulate metal oxides against peri-implantitis pathogens. *Int J Antimicrob Ag*. 2012;40(2):135–139.
11. Pati R, Mehta RK, Mohanty S, et al. Topical application of zinc oxide nanoparticles reduces bacterial skin infection in mice and exhibits antibacterial activity by inducing oxidative stress response and cell membrane disintegration in macrophages. *Nanomedicine*. 2014;10(6): 1195–1208.
12. Verma R, Naik KK, Gangwar J, et al. Morphology, mechanism and optical properties of nanometer-sized MgO synthesized via facile wet chemical method. *Mate Chem Phys*. 2014;148(3):1064–1070.
13. Sirelkhatim A, Mahmud S, Seeni A, et al. Review on zinc oxide nanoparticles: Antibacterial activity and toxicity mechanism. *Nano-Micro Lett*. 2015;7(3):219.
14. Allaker RP. The use of nanoparticles to control oral biofilm formation. *J Dent Res*. 2010;89(11):1175–1186.
15. Gordon T, Perlstein B, Houbara O, et al. Synthesis and characterization of zinc/iron oxide composite nanoparticles and their antibacterial properties. *Colloids Surf A*. 2011;374(1):1–8.
16. Abdel Rahman AT, Hafez SF, Abdelhakam SM, et al. Antimicrobial resistant bacteria among health care workers in intensive care units at Ain Shams University Hospitals. *J Egypt Soc Parasitol*. 2010; 40(1):71.
17. Saxena N, Dadhich D, Maheshwari D. Aerobic bacterial isolates from burn wound infection patients and their antimicrobial susceptibility pattern in Kota, Rajasthan. *J Evol Med Dent Sci*. 2013;23(2): 4156–4160.
18. Appelgren P, Bjornhagen V, Bragderyd K, et al. Prospective study of infections in burn patients. *Burns*. 2002;28(1):39–46.
19. Falagas ME, Bliziotis IA. Drug-resistant gram-negative bacteria: the dawn of the post-antibiotic era? *Int J Antimicrob Agents*. 2007;4: 191–198.
20. Martin JM, Zenilman JM, Lazarus GS. Molecular microbiology: new dimensions for cutaneous biology and wound healing. *J Invest Dermatol*. 2010;130(1):38–48.
21. Cooper M, Sarabahi S, Tiwari V, et al. Fungal infections in burns: diagnosis and management. *Indian J Plast Surg*. 2010;43 (Suppl):S37–S42.
22. Morsy R, Ali SS, El-Shetehy M. Development of hydroxyapatite-chitosan gel sunscreen combating clinical multidrug-resistant bacteria. *J Mol Struct*. 2017;1143:251–258.
23. Shirtliff ME, Peters BM, Jabra-Rizk MA. Cross-kingdom interactions: *Candida albicans* and bacteria. *FEMS Microbiol Lett*. 2014; 299(1):1–8.
24. Harriott MM, Noverr MC. Importance of *Candida*-bacterial polymicrobial biofilms in disease. *Trends Microbiol*. 2011;19(11):557–563.
25. Bertesteanua S, Triaridis S, Stankovic M, et al. Polymicrobial wound infections: pathophysiology and current therapeutic approaches. *Int J Pharm*. 2014;463(2):119–126.
26. Seth AK, Geringer MR, Hong SJ, et al. In vivo modeling of biofilm-infected wounds: a review. *J Surg Res*. 2012;178(1):330–338.
27. Grice EA, Snitkin ES, Yockey LJ, et al. Longitudinal shift in diabetic wound microbiota correlates with prolonged skin defense response. *Proc Natl Acad Sci U S A*. 2010;107(14):799–804.
28. Scott JA, Untereinen WA. Determination of keratin degradation by fungi using keratin azure. *Med Mycol*. 2004;42(3):239–246.
29. Hao YJ, Montiel R, Nascimento G, et al. Identification and expression analysis of the *Steinernema carpocapsae* elastase-like serine protease gene during the parasitic stage. *Exp Parasitol*. 2009;122(1):51–60.
30. Church D, Elsayed S, Reid O, et al. Burn Wound Infections. *Clin Microbiol Rev*. 2006;19(2):403–434.
31. Tapia DMT, Simões MLG. Production and partial characterization of keratinase produced by a microorganism isolated from poultry processing plant wastewater. *Afr J Biotechnol*. 2008;7(3):296–300.
32. Cao Z, Zhang Q, Chen W, et al. Characterization of a novel *Stenotrophomonas* isolate with high keratinase activity and purification of the enzyme. *J Indian Microbiol Biotechnol*. 2009;36(2):181–188.
33. Tainwala R, Sharma YK. Pathogenesis of dermathophytose. *Indian J Dermatol*. 2011;56(3):259–261.
34. Nagaharika Y, Kalyani V, Rasheed S, et al. Anti-inflammatory activity of leaves of *Jatropha gossypifolia* L. by HRBC membrane stabilization method. *J Acute Dis*. 2013;2(2):156–158.
35. Nagajyothi PC, Cha SJ, Yang IJ, et al. Antioxidant and anti-inflammatory activities of zinc oxide nanoparticles synthesized using *Polygala tenuifolia* root extract. *J Photochem Photobiol B*. 2015;146:10–17.
36. Peterson LR. Squeezing the antibiotic balloon: the impact of antimicrobial classes on emerging resistance. *Clin Microbiol Inf*. 2005; 11 (Suppl 5):4–16.
37. Dizaj SM, Lotfipour F, Barzegar-Jalali M, et al. Antimicrobial activity of the metals and metal oxide nanoparticles. *Mater Sci Eng*. 2014;44:278–284.
38. Escobedo-Morales A, Esparza R, García-Ruiz A, et al. Structural and vibrational properties of hydrothermally grown ZnO₂ nanoparticles. *J Cryst Growth*. 2011;316(1):37–41.
39. Siddiqui H, Qureshi MS, Haque FZ. Surfactant assisted wet chemical synthesis of copper oxide (CuO) nanostructures and their spectroscopic analysis. *Optik*. 2016;127(5):2740–2747.
40. Ahmadi MK, Vossoughi M. Immobilization of α-chymotrypsin on the curface of magnetic/gold core/shell nanoparticles. *J Nanotechnol*. 2013;2013, Article ID 830151, 7 pages.
41. Cheng S, Yan D, Chen JT, et al. Soft template synthesis and characterization of ZnO₂ and ZnO hollow spheres. *J Phys Chem C*. 2009; 113(31):13630.
42. Forbes BA, Sahm DF, Weissfeld AS. *Bailey and Scotts' Diagnostic Microbiology*. 12th ed., St. Louis, MO: Elsevier; 2007.
43. Graf B, Adam T, Zill E. U.B. Gobel, evaluation of the VITEK 2 system for rapid identification of yeasts and yeast-like organisms. *J Clin Microbiol*. 2000;38(5):1782–1785.
44. McClenny N. Laboratory detection and identification of *Aspergillus* species by microscopic observation and culture. *J Mo Mycol*. 2005; 43(Supp1):S125–S128.
45. Kreger-Van Rij NJW. *The Yeasts: A Taxonomic Study*. 3rd ed. Amsterdam, The Netherlands: Elsevier Science Publishers B.V.; 1984.

46. Yticesoy M, Marol S. Performance of chrom agar candida and biggy agar for identification of yeast species. *Annals Clin Microbiol Antimicrob*. 2003;2(8):1–7.

47. Bauer AWWMM, Kirby JC, Truck SM. Antibiotic susceptibility testing by a standardized single disk method. *Am J Clin Pathol*. 1966; 45(4):493–496.

48. European Committee for Standardization. European standard EN 1275: chemical disinfectants and antiseptics. Basic fungicidal activity. Test method and requirements (phase1). Brussels: Comite´ Europe´en de Normalisation; 1997.

49. Clinical and Laboratory Standards Institute. Performance standards for antimicrobial susceptibility testing; 24th informational supplement. CLSI document M100-S24. Wayne, PA: Clinical and Laboratory Standards Institute; 2014.

50. Lalitha P, Arathi KA, Shubashini K, et al. Antimicrobial activity and phytochemical screening of an ornamental foliage plant, *Pothos aurea* (Linden ex Andre). *An Int J Chem*. 2010;1(2):63–71.

51. Ohman DE, Cryz SJ, Iglewski BH. Isolation and characterization of *Pseudomonas aeruginosa* PAO mutant that produces altered elastase. *J Bacteriol*. 1980;142(3):836–842.

52. Blanco JL, Hontecillas R, Bouza E, et al. Correlation between the elastase activity index and invasiveness of clinical isolates of *Aspergillus fumigatus*. *J Clin Microbiol*. 2002;40(5):1811–1813.

53. Wawrzkiewicz K, Wolski T, Lobarzewski J. Screening the keratinolytic activity of dermatophytes in vitro. *Mycopathologia*. 1991; 114(1):1–8.

54. Joshi S, Tejashwini M, Revati N. Isolation, identification and characterization of a feather degrading bacterium. *Int J Poult Sci*. 2007; 6:689–693.

55. Shinde U, Phadke A, Nari A, et al. Membrane stabilization activity a possible mechanism of action for the anti-inflammatory activity of *Cedrusde odara* wood oil. *Fitoterapia*. 1999;70:251–257.

56. Gandhidasan R, Thamaraichelvan A, Baburaj S. Anti-inflammatory action of *Lannea coromandelica* by HRBC membrane stabilization. *Fitoterapia*. 1991;62(2):81–83.

57. Morris T, Stables M, Hobbs A, et al. Effects of low-dose aspirin on acute inflammatory responses in humans. *J Immunol*. 2009;183(3): 2089–2096.

58. Ahmadi MK, Fang L, Moscatello N, et al. *E. coli* metabolic engineering for gram scale production of a plant-based anti-inflammatory agent. *Metab Engin*. 2016;38:382–388.

59. Mizushima Y, Kobayashi M. Interaction of anti-inflammatory drugs with serum proteins, especially with some biologically active proteins. *J Pharm Pharm*. 1968;20(3):169–173.

60. Sakat S, Juvekar A, Gambhire M. In vitro antioxidant and anti-inflammatory activity of methanol extract of *Oxalis corniculata* Linn. *Int J Pharm Sci*. 2010;2(1):146–155.

61. Guo PC, Dong Z, Xiao L, et al. Silk gland-specific proteinase inhibitor serpin16 from the *Bombyx mori* shows cysteine proteinase inhibitory activity. *Biochem Biophy Res Co*. 2015;457(1):31–36.

62. El-Zawawy N, Ali SS. Pyocyanin as anti-tyrosinase and anti-tinea corporis: a novel treatment study. *Microb Pathogenesis*. 2016;100: 213–220.

63. Mohammadi-Samani S, Kouroshfard S, Azarpira N. Effects of phosphate supplementation on *Pseudomonas aeruginosa* invasive behavior in burn wound infections: a simple approach to a big problem. *Burns*. 2016;42(2):428–433.

64. Mousa HA. Aerobic, anaerobic and fungal burn wound infections. *J Hosp Infect*. 1997;37(4):317–323.

65. Li GH. Analysis of microbiological flora in the blood and wounds of burn patients. *Chung-Hua Cheng Hsing Shao Wai Ko Tsa Chih*. 1989; 5(3):238–239.

66. Husain MT, Karim QN, Tajuri S. Analysis of infection in a burn ward. *Burns*. 1989;15(5):299–302.

67. Donati L, Scamazzo F, Gervasoni M, et al. Infection and antibiotic therapy in 4000 burned patients treated in Milan, Italy, between 1976 and 1988. *Burns*. 1993;19(4):345–348.

68. Guangxia X, Dewang W, Yaping Z, et al. Early diagnosis of burn wound infection with aspergillus by the use of tissue sliver culture. In: Tisheng C, Jixiang S, Zhijun Y, editors. *Recent Advances in Burns and Plastic Surgery-The Chinese Experience*. Lancaster: MTP Press Ltd.; 1985:287–290.

69. Chakrabarti A, Nayak N, Kumar PS, et al. Surveillance of nosocomial fungal infections in a burn care unit. *Infection*. 1992;20(3):132–135.

70. Andrade F, Rafael D, Videira M, et al. Nanotechnology and pulmonary delivery to overcome resistance in infectious diseases. *Adv Drug Deliver Rev*. 2013;65(13):1816–1827.

71. Nagajyothi PC, MinhAn TN, Sreekanth TVM, et al. Green route biosynthesis: characterization and catalytic activity of ZnO nanoparticles. *Mater Lett*. 2013;108:160–163.

72. Sangeetha N, Kumaraguru AK. Extracellular synthesis of zinc oxide nanoparticle using seaweeds of gulf of Mannar. *India J Nanobiotechnol*. 2013;11(1):39.

73. Barker KS, Rogers PD. Recent insights into the mechanisms of antifungal resistance. *Curr Infect Dis Rep*. 2006;8(6):2816–2823.

74. Gauwerky K, Borelli C, Korting HC. Targeting virulence: a new paradigm for antifungals. *Drug Discov Today*. 2009;14(3):214–222.

75. Voltan AR, Donofrio F, Miranda ET, et al. Induction and secretion of elastinolytic and proteolytic activity in cultures of *Paracoccidioides brasiliensis*. *J Basic Appl Pharm Sci*. 2008;29:97–106.

76. Okumura Y, Ogawa K, Uchgiya K, et al. Characterization and primary structure of elastase inhibitor, AFLEI from *Aspergillus flavus*. *Jpn J Med Mycol*. 2007;48(1):13–18.

77. Santos ALS, Palmeira VF, Rozental S, et al. Biology and pathogenesis of *Fonsecaeaa pedrosoi*, the major etiologic agent of Chromoblastomycosis. *FEMS Microbiol Rev*. 2007;31(5):570–591.

78. Bruton LL. *Goodman and Gilman's Pharmacological Basis of Therapeutics*. 11th ed. New York: McGrew Hill; 2005:1102–1104.

79. Rosa MD, Giroud JP, Willoughby DA. Studies on the mediators of the acute inflammatory response induced in rats in different sites by carrageenan and turpentine. *J Pathol*. 1971;104(1):15–29.

80. Das SN, Chatterjee S. Long term toxicity study of ART-400, *Indian Indg Med*. 1995;16(2):117–123.

81. Fuller FW. The side effects of silver sulfadiazine. *J Burn Care Res*. 2009;30(3):464–470.

82. Rashaan ZM, Krijnen P, Klamer RR, et al. Non-silver treatment versus silver sulfadiazine in treatment of partial thickness burn wounds in children: a systematic review and meta-analysis. *Wound Repair Regen*. 2014;22(4):473–482.
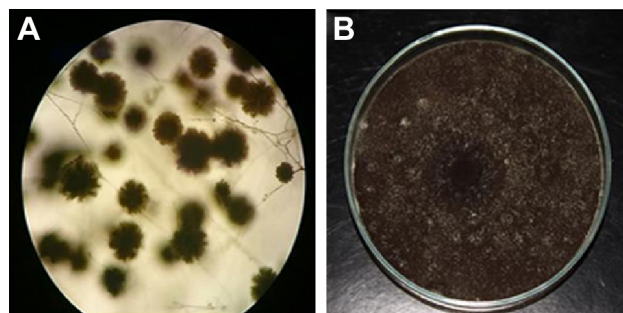
Supplementary materials

Figure S1 Microscopic (**A**) and macroscopic (**B**) examination of *Aspergillus niger*.
Notes: For microscopic examination, magnification power is (40×) and scale bar is 2 mm.

Table S1 In vivo evaluation of inflammation, ulcer formation, and re-epithelialization in different rabbit groups

Rabbit group (n=6)	Inflammation	Surface ulceration	Re-epithelialization
Group 1 (negative control)	+	+	Partial
Group 2 (positive control)	+	+	–
Group 3 (ZnO$_2$-NPs-receiving group)	–	–	Complete
Group 4 (silver sulfadiazine-receiving group)	+	+	–

Notes: –, absent; +, present.
Abbreviation: NPs, nanoparticles.